

Quantum and Thermal Effects in H₂ Dissociative Adsorption: Evaluation of Free Energy Barriers in Multidimensional Quantum Systems

Greg Mills and Hannes Jónsson

Department of Chemistry, BG-10, University of Washington, Seattle, Washington 98195

(Received 2 August 1993)

We have evaluated the sticking probability and activation energy for dissociation of H₂ molecules on a Cu(110) surface by a reversible work formulation of quantum transition state theory. Feynman path integrals are used to describe the two hydrogen atoms and a few of the surface atoms, thereby including quantum effects such as tunneling and zero point energy, as well as thermal averaging. At a temperature below 600 K an onset of a quantum regime is observed as the activation energy drops by 30%.

PACS numbers: 82.65.Pa, 05.30.-d, 68.35.Md, 82.65.My

The dissociative adsorption of molecules on surfaces of solids is of central importance in surface catalysis and has been extensively studied both experimentally and theoretically. Hydrogen adsorption on copper surfaces has become "the classic example of activated dissociative adsorption of a molecule at a surface" [1]. Many experiments have made use of molecular beams with molecules in a selected initial state impinging on the surface. The theoretical studies have focused on classical trajectory simulations and quantum wave-packet propagation to explore the dissociative sticking dynamics given a well defined initial state of the molecule [1]. A great deal of qualitative insight has been gained, but many questions remain open. On the theoretical side, the problem is that full quantum mechanical treatment of all six hydrogen degrees of freedom is impractical with present computers and currently available techniques for quantum wave-packet propagation. The theoretical work has therefore largely been confined to lower-dimensional model systems [1,2]. Not only is a six-dimensional wave-packet propagation a big order, but such a calculation would need to be repeated multiple times to average over the surface vibrational degrees of freedom to get a single value of the sticking probability. Low dimensional simulations have demonstrated clear quantum effects [1,2] and calculations in higher (up to four) dimensions, have indicated that dimensional effects might be equally important [3,4]. It has been hypothesized that if quantum calculations could be extended to include many more degrees of freedom, then results from classical and quantum calculations would be similar, due to the increased degree of averaging in higher dimensions [5].

We report here on a fully quantum and thermally averaged simulation of the dissociative sticking of H₂ on Cu(110). The large number of degrees of freedom can be included at the expense of the amount of detail obtained about the dynamics. We use the statistical Feynman path integral (FPI) technique which implicitly performs the thermal averaging over quantum states. The simulation mimics a thermodynamic experiment, where the impinging molecules have a thermal energy distribution at the temperature of the substrate. This experiment has been carried out in the laboratory of Campbell and co-

workers [6,7] who obtained the thermodynamic activation barrier for dissociative adsorption from the temperature dependence of the sticking probability. Our simulations show a clear onset of a quantum mechanical regime as the activation energy drops by 30% at a temperature below 600 K. The experimental measurements fall in the vicinity of this transition temperature, but are taken over too narrow a temperature range to show the transition.

The FPI formalism has been used to study equilibrium quantum statistical properties of various systems [8-12]. An isomorphism is exploited between the quantum statistics of the system and the purely classical statistics of cyclic chains of images of the quantum particles coupled by harmonic springs [13]. The spring constant of the chains is $mP/\hbar^2\beta^2$ where m is the particle mass and $\beta=1/k_B T$. Gillan used this to study the diffusion of a hydrogen atom in a metal [14,15]. He evaluated the activation free energy barrier by calculating the mean force \mathbf{f} on the FPI chain while holding its centroid fixed at various points along a path leading up to the saddle point of the potential energy surface. The free energy difference was obtained from the reversible work, $\Delta F = -\int ds \cdot \mathbf{f}$. This method can be thought of as a quantum mechanical transition state theory (TST) [14,15]. The basic idea of treating the coordinates of the centroid of the FPI as classical variables has subsequently been used to generalize formulations of classical TST to quantum systems [14, 16]. There the transition rate is obtained by evaluating the density of the centroid at a dividing surface by Monte Carlo sampling. These methods have been applied to several problems involving transitions in one-, two-, and three-dimensional quantum systems, such as collinear H+H₂ reaction [14] and hydrogen diffusion on a surface [17]. The results were shown to be in good agreement with more accurate dynamics calculations.

It is important to keep in mind the least restrictive assumptions made in classical TST [18,19]. First, the transition rate is assumed to be low enough that a Boltzmann distribution of energy is maintained in the various degrees of freedom of the *reactants*. Second, a bottleneck is assumed to exist in phase space which allows the definition of a dividing surface clearly separating reactants from products. The central approximation is the assumption

that if a trajectory crosses this dividing surface in the direction from reactant to product, it will end up on the product side for a long time. Since recrossings are neglected, the classical TST estimate is always an upper bound to the exact classical rate, a principle exploited in variational TST to find the optimal dividing surface. While TST is usually applied to problems involving substantial energy barriers, these are not required. For example, the theory correctly predicts the rate of effusion of ideal gas through a small hole of a container, a problem involving only an entropic barrier.

We have extended Gillan's reversible work quantum TST method to better account for transitions involving two or more quantum particles and transitions involving curved reaction paths. In the course of the reversible work evaluation an optimal dividing surface is determined and the method reduces to a variational TST in the classical limit [15]. Here we apply the method to study the dissociative adsorption of H_2 molecules on a Cu(110) surface, a two quantum particle transition.

The potential surface for the H_2 -Cu system was modeled in a simple way, using an embedded atom method (EAM) type form [20] $V(\mathbf{R}) = \sum_i \sum_j \phi(r_{ij}) + \sum_i E(\rho_i)$ with $\rho_i = \sum_{j \neq i} \rho_j^A(r_{ij})$. Here ϕ is a pairwise interaction, and ρ^A is an atomic electron density, both modeled by double exponentials. The embedding function $E(\rho)$ is a polynomial. This form was chosen because it allows fast computations, only roughly a factor of 2 slower than simple pairwise potentials. The qualitative shape of the potential was tailored after the LEPS type potential of Lee and DePristo [21]. It has a late saddle point for adsorption, which is consistent with the experimentally measured enhancement of the sticking coefficient by vibrational excitation [22,23]. The potential barrier, however, was scaled up to 0.73 eV to match the estimate of Hand and Harris based on *ab initio* calculations [24]. The binding energy of the H atoms on the surface was adjusted to be 0.23 eV, deduced from the difference in activation energies of adsorption and desorption [25], making the adsorption process endothermic by 0.2 eV. The H_2 dimer potential matches the binding energy, distance, and vibrational frequency of the exact *ab initio* potential to within 1%. A contour plot of the potential for adsorption at the long bridge is shown in Fig. 1.

In order to carry out the evaluation of the free energy barrier, the following is needed: (1) A smooth and continuous transition of the system from the reactant to the product state. (2) A five-dimensional transition state dividing surface. (3) An evaluation and integration of the mean force on the system to get the reversible work involved in driving the system from the reactant state to the transition state. For the first item, we have used the minimum energy path, determined by applying a technique we refer to as "nudged elastic band" method [26]. We then define a sequence of perpendicular, five-

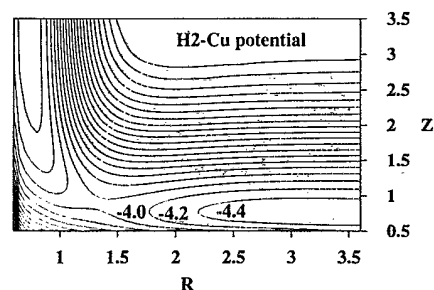


FIG. 1. Potential energy contours for the dissociation of H_2 on Cu(110). In this two-dimensional cut through the six-dimensional potential surface the molecule is coming down parallel to the surface, symmetrically arranged over a long bridge site. The saddle point energy is 0.729 eV.

dimensional hyperplanes bringing the hydrogen atoms gradually from the initial molecular state to the atomic chemisorbed state. The average force acting on the hydrogen atoms in each of the hyperplanes was obtained by carrying out a molecular dynamics simulation with the centroids of the hydrogen atom FPIs constrained to remain in the hyperplane. More specifically, a six-dimensional unit vector $\hat{\Gamma}_{\parallel}$ in the direction of the path is used to constrain the dynamics. At each time step the component of the net force on the FPI images normal to the hyperplane, $\mathbf{f} \cdot \hat{\Gamma}_{\parallel}$, is collected for the evaluation of the thermal average $\langle \mathbf{f}_{\parallel} \rangle$. This component is then projected out of the force on the images to give a new, revised force such that $\mathbf{f}^{\text{new}} \cdot \hat{\Gamma}_{\parallel} = 0$. The centroids of the FPI chains then remain in the hyperplane. We have used the velocity Verlet algorithm to carry out the molecular dynamics [27]. The constrained dynamics conserve energy as long as the constraint vector is constant. We define the transition state to be the hyperplane where $\langle \mathbf{f}_{\parallel} \rangle = 0$. In general, the orientation of the hyperplanes at and near the transition state might need to be adjusted. We found this to be a very minor effect in the present case. The classical limit is easily obtained in this formalism, as each chain gradually shrinks into a single atom.

Figure 2 shows the change in the potential energy along the reaction path and the classical and quantum mechanical free energy obtained at $T=100$ K. In addition to the hydrogen atoms, the eight nearest Cu atoms are also included as FPI chains, each with fifty images. As the molecule approaches the surface, the classical free energy initially rises above the potential energy due to a drop in the entropy as the molecular orientation becomes confined. Eventually, in the transition state hyperplane, the spread in the polar angle and in the azimuthal angle is down to ca. $\pm 10^\circ$. Closer to the surface the H_2 vibration softens leading to increased vibrational entropy. At the transition state the two effects have largely canceled in the classical simulation. The quantum simulation shows that delocalization (tunneling and zero point ener-

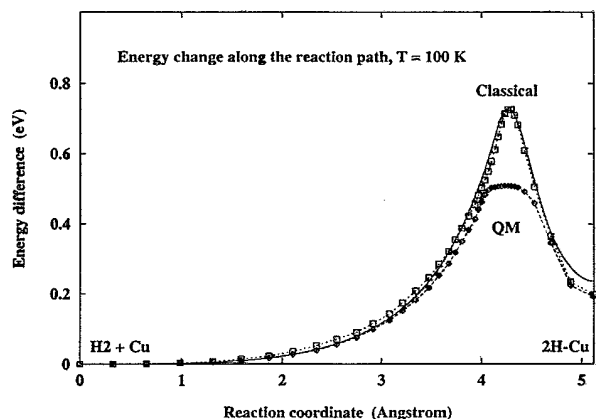


FIG. 2. The changes in the potential energy (solid line) and the classical (squares) and quantum (diamonds) free energy along the reaction path at $T=100$ K. The zero for each of the three curves is arbitrarily chosen to be when the molecule is far from the surface.

gy effects) results in 0.2 eV lowering of the free energy barrier at this temperature (see Fig. 2).

Figure 3 shows the temperature dependence of the calculated free energy barrier for dissociative sticking. The slope gives the effective activation energy $E_a = \partial(\beta\Delta F)/\partial\beta$. At $T=600$ K the classical and quantum free energy curves coincide along the entire reaction path; the string of beads in the quantum description has largely collapsed into a point which then behaves as a classical atom. Below 600 there is a clear onset of quantum behavior as the activation energy drops from 0.70 to 0.45 eV. This is due to the delocalization of the H atoms, which is evident from spreading of the FPI chains. The temperature at which the springs are loose enough to allow the chains to spread is directly related to the curvature κ of the potential barrier along the reaction path [13] $T_c = (\hbar/2\pi)\sqrt{\kappa/m}$. From the curvature of our model potential this estimate gives $T_c = 5 \times 10^2$ K, very close to the transition temperature observed in the simulations.

Also shown in Fig. 3 are the experimental data taken by Campbell and co-workers [7]. Those fall in the vicinity of the transition region. The inset shows on an expanded scale the experimental data points and the lines fitted to the simulated results. To facilitate the comparison of the slopes the experimental data has been shifted down. The slope and therefore the activation energy and even the change in slope of the simulated data at the onset of the quantum regime are consistent with the experimental measurements. For D_2 Campbell and co-workers found slightly higher activation energy, by 0.06 eV. Our simulations give a value higher by 0.08 eV in the quantum region (see Fig. 3).

We have also evaluated the free energy barrier for desorption as a function of temperature. This was measured by Anger, Winkler, and Rendulic [25] at around 300 K to be 0.43 eV in the limit of zero coverage. Our

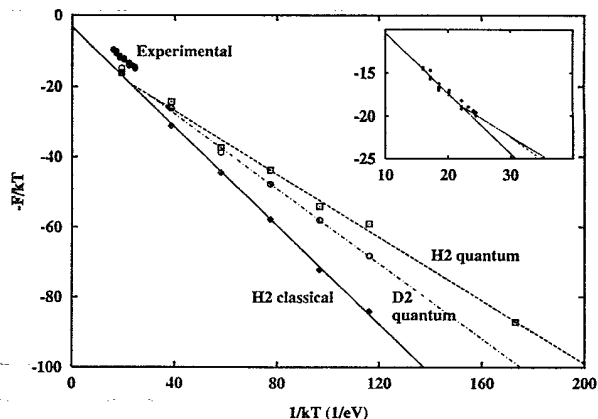


FIG. 3. The calculated free energy barrier for dissociative sticking using quantum representation of H_2 (open squares), quantum representation of D_2 (open circles), and classical representation of H_2 (open diamonds), as a function of inverse temperature. The slope of the curves gives the effective activation energy. At $T=600$ K the classical and quantum simulations of H_2 are nearly identical. Below 600 K there is a clear onset of quantum behavior with 30% lower activation energy due to tunneling and zero point motion effects. The experimental measurements (solid circles) land close to the transition temperature. The inset shows the best fit lines through the calculations and the experimental data on an expanded scale. To facilitate the comparison of the slopes, the experimental data have been shifted down by 0.49.

simulations give 0.38 eV in a comparable temperature range, indicating the chemisorption bond is slightly too weak in our model potential surface.

While the calculated and measured activation energy is in good agreement, the measured sticking coefficient [7] at 600 K is 4×10^{-6} , larger than our calculated value, $\exp(-\beta\Delta F) = 1 \times 10^{-7}$. This suggests the entropic barrier in our simulations is too high, i.e., the transition state region of the model potential surface, which was modeled after the LEPS form, is too confined.

In order to estimate the effect of vibration and rotation, we repeated the simulations without vibrational and rotational degrees of freedom of the hydrogen molecule. In the classical simulation each one of the H atoms is held fixed during the calculation of the mean force. In the quantum simulation each of the two hydrogen atom centroids is held fixed (see Fig. 4), i.e., six constraints are applied to the system rather than one as in the hyperplane dynamics. The quantum simulation still includes effects due to delocalization because the images have substantial freedom to wander away from the centroid. The activation energy changed only slightly: 0.03 eV higher for both the quantum and classical case. This is consistent with the conclusion of Campbell and co-workers [7] and others [28] that even though vibrationally excited molecules have substantially higher sticking probability, the population of the excited levels in a Boltzmann distribution at these temperatures is so low that the net enhance-

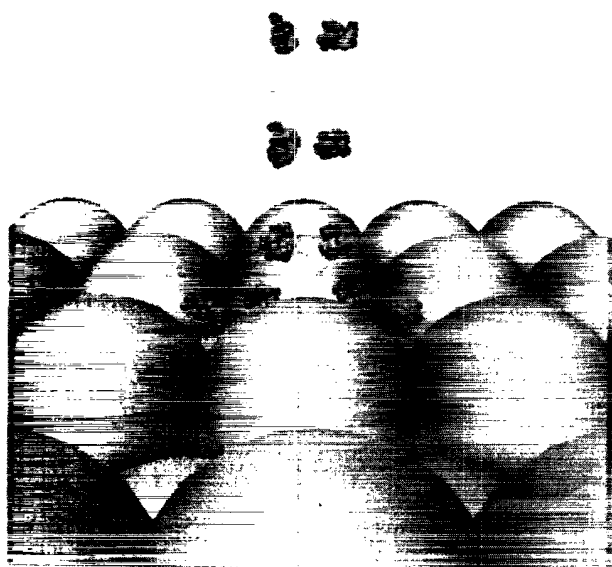


FIG. 4. Snapshot from the quantum mechanical free energy calculation at $T=300$ K with fixed centroids (six constraints) at five points along the minimum energy path. The mean force on the images is evaluated in the simulation. The distribution of the H atom images indicates the extent of quantum delocalization.

ment is negligible. This also shows the net effect of vibrational and rotational zero point motion is small, a conclusion also reached by Müller [29]. The 30% lowering of the activation energy in the quantum regime is primarily due to H atom tunneling.

We thank Art Voter and Greg Schenter for enlightening discussions about transition state theory and its extensions to quantum systems. Numerous discussions with Charlie Campbell on the dissociative sticking problem have been very valuable. This work was supported by the Division of Chemical Sciences, Office of Basic Energy Research, U.S. Department of Energy, under Grant No. DE-FG06-91ER14224. Greg Mills is a Hertz foundation graduate fellow.

[1] See contributions by J. Harris, A. E. DePristo, S. Holloway, and B. E. Hayden, in *Dynamics of Gas-Surface Interactions*, edited by C. T. Rettner and M. N. R. Ashfold (The Royal Society of Chemistry, Cambridge, 1991).

[2] B. Jackson and H. Metiu, *J. Chem. Phys.* **86**, 1026 (1986).

- [3] C. Engdahl and U. Nielsen, *J. Chem. Phys.* **98**, 4223 (1993).
- [4] U. Nielsen, D. Halstead, S. Holloway, and J. K. Norskov, *J. Chem. Phys.* **93**, 2879 (1990).
- [5] See p. 95 in Ref. [1].
- [6] J. M. Campbell, M. E. Domagala, and C. T. Campbell, *J. Vac. Sci. Technol. A* **9**, 1693 (1991); J. M. Campbell and C. T. Campbell, *Surf. Sci.* **259**, 1 (1991).
- [7] M. Parrinello and A. Rahman, *J. Chem. Phys.* **80**, 860 (1984).
- [8] J. A. Barker, *J. Chem. Phys.* **70**, 2914 (1979).
- [9] D. Chandler and P. G. Wolynes, *J. Chem. Phys.* **74**, 4078 (1981).
- [10] J. D. Doll and D. L. Freeman, *J. Chem. Phys.* **80**, 2239 (1984).
- [11] M. Sprik, R. Impey, and M. L. Klein, *Phys. Rev. Lett.* **56**, 2326 (1986).
- [12] M. J. Gillan, *Phys. Rev. Lett.* **58**, 563 (1987); *Philos. Mag. A* **58**, 257 (1988).
- [13] R. P. Feynman and A. R. Hibbs, *Quantum Mechanics and Path Integrals* (McGraw Hill, New York, 1965). See in particular pp. 280-286.
- [14] G. A. Voth, D. Chandler, and W. H. Miller, *J. Chem. Phys.* **91**, 7749 (1989).
- [15] The theoretical foundation of the method and detailed comparison with Gillan's method and centroid density methods is given by G. Schenter, G. Mills, and H. Jónsson (to be published).
- [16] M. Messina, G. K. Schenter, and B. C. Garrett, *J. Chem. Phys.* **98**, 8525 (1993).
- [17] Y-C. Sun and G. A. Voth, *J. Chem. Phys.* **98**, 7451 (1993); T. R. Mattsson, U. Engberg, and G. Wahnström, *Phys. Rev. Lett.* **71**, 2615 (1993).
- [18] D. Chandler, *J. Chem. Phys.* **68**, 2959 (1978).
- [19] A. F. Voter and J. D. Doll, *J. Chem. Phys.* **82**, 80 (1985).
- [20] M. S. Daw and A. M. Foiles, *Phys. Rev. B* **35**, 2128 (1987).
- [21] C-Y. Lee and A. E. DePristo, *J. Chem. Phys.* **85**, 4161 (1986).
- [22] B. E. Hayden and C. L. A. Lamont, *Phys. Rev. Lett.* **63**, 1823 (1989).
- [23] H. F. Berger and K. D. Rendulic, *Surf. Sci.* **253**, 325 (1991).
- [24] M. R. Hand and J. Harris, *J. Chem. Phys.* **92**, 7610 (1990).
- [25] G. Anger, A. Winkler, and K. D. Rendulic, *Surf. Sci.* **220**, 1 (1989).
- [26] H. Jónsson and G. Mills (to be published).
- [27] H. C. Andersen, *J. Chem. Phys.* **72**, 2384 (1980).
- [28] C. T. Rettner, H. A. Michelsen, and D. J. Auerbach, *Trans. Faraday Soc.* (to be published).
- [29] J. E. Müller, *Surf. Sci.* **272**, 45 (1992).